Development 129, 1273-1281 (2002)
Printed in Great Britain © The Company of Biologists Limited 2002
DEV5963

Control of *Drosophila* imaginal disc development by *rotund* and *roughened eye*: differentially expressed transcripts of the same gene encoding functionally distinct zinc finger proteins

Susan E. St Pierre[1], Maximo I. Galindo[2], Juan P. Couso[2,*] and Stefan Thor[1,*]

[1]Department of Neurobiology, Harvard Medical School, 220 Longwood Avenue, Boston, MA 02115, USA
[2]School of Biological Sciences, University of Sussex, Falmer, Brighton BN1 9QG, UK
*Authors for correspondence (e-mail: j.p.couso@biols.susx.ac.uk and sthor@hms.harvard.edu)

Accepted 26 November 2001

SUMMARY

The *Drosophila rotund* gene is required in the wings, antenna, haltere, proboscis and legs. A member of the Rac family of GTPases, denoted the *rotund racGAP* gene, was previously identified in the *rotund* region. However, previous studies indicated that *rotund racGAP* was not responsible for the *rotund* phenotypes and that the *rotund* gene had yet to be identified. We have isolated the *rotund* gene and show that it is a member of the *Krüppel* family of zinc finger genes. The adjacent *roughened eye* locus specifically affects the eye and is genetically separable from *rotund*. However, *roughened eye* and *rotund* are tightly linked, and we have therefore also isolated the *roughened eye* transcript. Intriguingly, we show that *roughened eye* is part of the *rotund* gene but is represented by a different transcript. The *rotund* and *roughened eye* transcripts result from the utilization of two different promoters that direct expression in non-overlapping domains in the larval imaginal discs. The predicted Rotund and Roughened Eye proteins share the same C-terminal region, including the zinc finger domain, but differ in their N-terminal regions. Each cDNA can rescue only the corresponding mutation and show negative effects when expressed in each others domain of expression. These results indicate that in addition to the differential expression of *rotund* and *roughened eye*, their proteins have distinct activities. *rotund* and *roughened eye* act downstream of early patterning genes such as *dachshund* and appear to be involved in *Notch* signaling by regulating *Delta*, *scabrous* and *Serrate*.

Key words: Imaginal disc development, Zinc finger, *Drosophila melanogaster*, Dual promoters, *rotund*, *roughened eye*

INTRODUCTION

The *Drosophila rotund* (*rn*) locus is recessive viable causing male and female sterility as well as defects in adult body structures (Cavener et al., 1986). These include defects in the antennae, wing, haltere and proboscis as well as fusion of all five leg tarsi into one fused tarsal-like segment. Analysis of third instar larvae imaginal discs revealed localized cell death in the regions giving rise to the affected adult structures (Kerridge and Thomas-Cavallin, 1988). The *rn* locus has previously been molecularly analyzed (Agnel et al., 1989) and a cDNA encoding a member of the Rac family of GTPase-activating proteins (GAP) was isolated from this genomic region (Agnel et al., 1992b). Since this gene was located in the *rn* genomic region it was denoted the *rotund racGAP* (*rnracGAP*), but molecular analysis of multiple *rn* alleles indicated that the *rnracGAP* is not responsible for the *rn* phenotypes (Agnel et al., 1992a). In fact, all studies to date instead point to an uncharacterized larger transcript as the likely candidate for the *rn* gene (Agnel et al., 1992a; Hoemann et al., 1996).

The closely linked *roughened eye* (*roe*) locus affects a late step in the development of the eye, and *roe* mutants display rough eye morphology and reduction of photoreceptors (Renfranz and Benzer, 1989). The *roe* gene is genetically separable from *rn*, but the two genes show complex complementation (Brand and Campos-Ortega, 1990; Kerridge and Thomas-Cavallin, 1988; Ma et al., 1996). This previously led to the suggestion that *rn* and *roe* may be 'two classes of mutation of the same gene, each of them disrupting a subfunction' (Ma et al., 1996). To address the tight link between these two adjacent loci we have isolated the *rn* and *roe* genes. Intriguingly, our results show that *roe* is part of the *rn* gene but is represented by a different transcript. These two transcripts encode predicted proteins with an identical C-terminal region, containing a Krüppel-type zinc finger domain, but with different N-terminal regions. *rn* and *roe* are expressed in non-overlapping domains in the larval imaginal discs. Each cDNA can rescue only the corresponding mutation and when misexpressed in each others domain of expression has negative effects. Our results indicate that these two loci are genetically separable not only because of their differential expression but also because of distinct activities of the Rn and Roe proteins. By analyzing the expression of a number of markers in the

developing imaginal discs, we further show that *rn* and *roe* act downstream of early patterning genes such as *dachshund*, but may act to modulate Notch signaling by regulating expression of Delta, Scabrous and Serrate.

MATERIALS AND METHODS

Fly stocks

w^{1118}, roe^{3}, *UAS-lacZ*, and p^{p},*cu* (Bloomington Stock Center); rn^{89} (Couso and Bishop, 1998) identified as P089 in Flyview stock collection (http//pbio07.uni-muenster.de); rn^{16}, rn^{19}, rn^{20} (Agnel et al., 1989); *sev-GAL4* (A. Bailey and G. M. Rubin); *GMR-GAL4* (Hay et al., 1997); *UAS-rn#1*, *UAS-rn#32*, *UAS-roe#18*, *UAS-roe#88* and $rn^{GAL4\#5}$ (this study). Mutations were maintained over standard balancers with *lacZ* or *GFP* markers.

Isolation of *rn* and *roe* cDNAs

Using genomic fragment D (Agnel et al., 1989) (provided by R. Griffin-Shea) as a probe, three *Drosophila* cDNA libraries were screened for a total of 11 million plaques and colonies. A larval λgt11 cDNA library (Clontech) yielded a 1.3 kilobase pair (kb) positive clone (4H). Comparison of the 4H sequence with *Drosophila* genomic sequence revealed that the 4H cDNA was truncated on both ends owing to internal *Eco*RI sites. To obtain the remainder of the cDNA we used PCR to amplify a 700 bp fragment downstream of the 3′ *Eco*RI site and used this PCR fragment to screen the same larval library. From 4 million plaques a 2.3 kb clone (22-4) was isolated and sequenced. The compiled cDNA sequence (4H/22-4) contained a long open reading frame (ORF) encoding a putative protein of 945 amino acids (aa; GenBank AF395905). There are several putative start codons at the beginning of the ORF, one of which closely matches the *Drosophila* consensus (Cavener and Ray, 1991). Owing to internal *Eco*RI sites at the 5′ of clone 4H and the 3′ of clone 22-4, the precise extent of the *rn* gene was not determined. Immediately 3′ of clone 22-4 the genome sequence reveals a number of polyadenylation sites that likely are used as termination signals.

We used a 3′ fragment from *rn* clone 22-4 (bp 2714-3658 of GenBank AF395905) as a probe to screen the larval cDNA library used for isolation of the *rn* cDNA. This yielded 2 positive clones out of 5 million plaques. Both clones contained truncated *roe* cDNAs, corresponding to bp 332-2856 and 621-2856 (GenBank AF395904). Both inserts crossed the junction between exon 1 and exon 2 of the predicted *roe* gene, extending past the end of the Roe ORF. Since we did not obtain a full-length *roe* cDNA, we verified the structure of the *roe* transcript by amplifying part of it using RT-PCR. For this, RNA from w^{1118} embryos was isolated and purified using RNAsol (Tel-Test, Inc.) and Qiagen Oligotex (Qiagen). We designed a primer in the predicted first exon, 5′ to stop codons in all three reading frames and followed by the predicted Roe start methionine (TAAAATTGTGCTTGGACCAGTGAA), and 2 primers in exon 2 (ATGCGAGAGCTGCGTGAACTT and TGCGACAGATACGACGAGTTGG). Using these primers, nested PCR was performed and a product of the predicted size was generated. Sequencing of this fragment was in agreement with our prediction for the intron/exon structure of *roe* (GenBank AF395904).

Generation of *UAS-rn* and *UAS-roe*

rn sequences corresponding to position 0-3373 (GenBank AF395905) of *rn* cDNA, and *roe* sequences corresponding to 0-2160 of *roe* cDNA (GenBank AF395904) and 86 bp of upstream genomic DNA, were cloned into the pUAST vector (Brand and Perrimon, 1993). Three independent *UAS-rn* and eight independent *UAS-roe* transgenic lines were generated using P-element transformation (Spradling and Rubin, 1982). These lines were tested for expression using *GMR-GAL4* and all gave strong phenotypes indicating similar levels of expression.

P-element analysis

The insertion of the rn^{89} enhancer trap, a *P[lArB]* insert, was determined using standard plasmid rescue methods. This revealed that *P[lArB]* is inserted at position –440 bp upstream of the *rn* cDNA (GenBank AF395905).

Conversion of *P[lArB]* in rn^{89} to *P[GawB]* was carried out as previously described (Sepp and Auld, 1999) with some modifications. Briefly, males of the genotype w^{1118}, $elav^{C155P[GawB]}$;;rn^{89}/*Δ2-3,Sb* were crossed to w^{1118} females and their progeny screened for red-eyed males (indicating that the *P[GawB]* had mobilized onto the autosomes). These males were crossed singly to *UAS-GFP/TM3,Sb* and their progeny screened for the *rn* expression pattern in larvae. From 30 lines screened, 3 independent insertions ($rn^{GAL4\#5}$, $rn^{GAL4\#13}$, $rn^{GAL4\#14}$) expressed GFP in the *rn* pattern and subsequently failed to complement *rn*. The site of insertion and the orientation of *P[GawB]* was determined by PCR amplification and sequencing. In all three cases *P[GawB]* was inserted in the exact same position as rn^{89} *P[lArB]*. For the rescue experiments $rn^{GAL4\#5}$ was used. The three rn^{GAL4} lines enhance the wing phenotype of Ser^{1}, common to many third chromosome balancer lines (not shown).

To verify that the rn^{89} and $rn^{GAL4\#5}$ mutant phenotypes were due to the insertion of the P elements, we excised them by standard methods. For rn^{89}, six independent revertants were isolated using their complementation of *rn*. Two independent revertant lines ($rn^{\#1–5}$ and $rn^{\#2–1}$) were homozygous viable and showed no *rn* phenotype. They were further analyzed by PCR and sequencing to determine the structure at the P-element insertion site. In both cases the P element had imprecisely excised but left a 30 bp ($rn^{\#1–5}$) and 37 bp ($rn^{\#2–1}$) 'footprint' containing the expected direct duplication of the 8 bp P-element target sequence and additional sequences from both ends of the P element. These 'footprints' are outside the identified *rn* exons thus explaining why they reverse the *rn* phenotype. Additionally, four stronger independent alleles were identified, one of which, $rn^{Δ2–2}$ was analyzed in more detail. Southern blot analysis using multiple probes, revealed that $rn^{Δ2–2}$ retained *P[lArB]* but is deleted for 3′ flanking genomic DNA removing the first and part of the second *rn* exon (Fig. 1A). For the reversion of $rn^{GAL4\#5}$ a similar strategy was used and we obtained 5 independent revertant lines that complemented multiple *rn* alleles, and in addition had lost the *white* marker and *GAL4* expression.

Analysis of *roe*^{3}

To identify the EMS-induced mutation in roe^{3}, we amplified a 1.5 kb genomic region covering the first exon of *roe* (primers were ATGCGAGAGCTGCGTGAACTT and CCAAATGGAAGGCCGTCTCA). Three independent PCR fragments using genomic DNA from w^{1118}, roe^{3}/rn^{20} and $p^{p}cu^{1}$ were sub-cloned and three clones from each were sequenced ($p^{p}cu^{1}$ was used as a second control since the roe^{3} parental chromosome could not be obtained). We found several conservative changes between roe^{3} and each of the other two lines, but only one non-conservative change between roe^{3} and both w^{1118} and $p^{p}cu^{1}$. This was a nonsense C→T mutation resulting in a glutamine to amber stop codon change at aa position 191 (bp 629 in GenBank AF395904) in the Roe ORF (Fig. 1A). This mutation would truncate the predicted Roe protein and the mutant protein would lack the entire C-terminal region including the ZF domain.

In situ hybridization and immunohistochemistry

Standard in situ protocols were used to examine expression of *rn* and *roe* (Tautz and Pfeile, 1989). We used three probes, 4H, containing *rn*-only sequences (0-1331of GenBank AF395905), *roe*, containing the first exon of *roe* (0-785 of GenBank AF395904) and ZF, containing common 3′ sequences including the ZF domain (2016-3373 of GenBank AF395905). Sense probes showed no signal in embryos or larvae. For the roe rescue experiments, adult eyes were cryo-sectioned and immunostained for Elav, a marker for photoreceptors (O'Neill et al., 1994). More than 14 ommatidia from more than four flies per genotype were analyzed and the total number

of R1-7 photoreceptors determined. For epistatic analysis, third instar imaginal discs were immunostained using the following primary antibodies: anti-Elav (1:10), anti-Dac (1:25), anti-Boss (1:2000), anti-Sca (1:10), anti-Ser (1:1000), anti-Bab (1:2000) and anti-Dl (1:20).

RESULTS

Isolation of rotund and roughened eye

To isolate the *rn* cDNA we used genomic fragment D (Fig. 1A), shown to hybridize to the putative *rn* transcript (Agnel et al., 1989). The cDNA sequence indicates that *rn* encodes a Krüppel-type zinc finger (ZF) protein and contains six C_2H_2 ZFs. The predicted Rn protein has a high degree of homology to the predicted protein of *Drosophila* gene CG5557 (Adams et al., 2000), and to *C.elegans* Lin-29 (Rougvie and Ambros, 1995). Over the ~150 aa ZF domain these two proteins display 84-90% identity to Rn (Fig. 1C). Among mammalian proteins, a recently identified rat cDNA, Cas-Interacting Zinc finger (CIZ) (Nakamoto et al., 2000), displays the highest homology (59% in the ZF) to Rn. Rn and CG5557 also share a short C-terminal domain of high homology not found in the other proteins (Fig. 1C). In line with the complex genetics of this area, the alignment of the *rn* cDNA with the genomic sequence reveals that *rn* spans ~50 kb and extends on both sides of the *rnracGAP* (Fig. 1A).

The *roe* gene shows complex complementation with *rn* and a number of *roe* alleles are also *rn* (Agnel et al., 1989; Brand and Campos-Ortega, 1990; Kerridge and Thomas-Cavallin, 1988; Ma et al., 1996). The *rn* gene structure together with previous molecular work on *rn* alleles gave us some initial insight into the identity of *roe*. Particularly informative were the $rn^{\Delta 2-2}$ and rn^{19} alleles. The $rn^{\Delta 2-2}$ P-element excision allele (materials and methods) contains a deletion in the *rn* 5′ region removing the first and part of the second exon of *rn* (Fig. 1A). Complementation analysis of $rn^{\Delta 2-2}$ shows that it is a null allele of *rn* but does not cause *roe* phenotypes (see below). Furthermore, the rn^{19} allele, shown to contain a larger deletion in the *rn* 5′ region (Agnel et al., 1989), acts as a *rn* null allele and, although it removes at least one other lethal complementation group, does not cause *roe* phenotypes. These results indicated the existence of *roe*-specific functions encoded in the genomic region proximal to the breakpoint of rn^{19} (Fig. 1A). One model could be the existence of *roe* specific exon(s) that are spliced and utilized specifically in the eye.

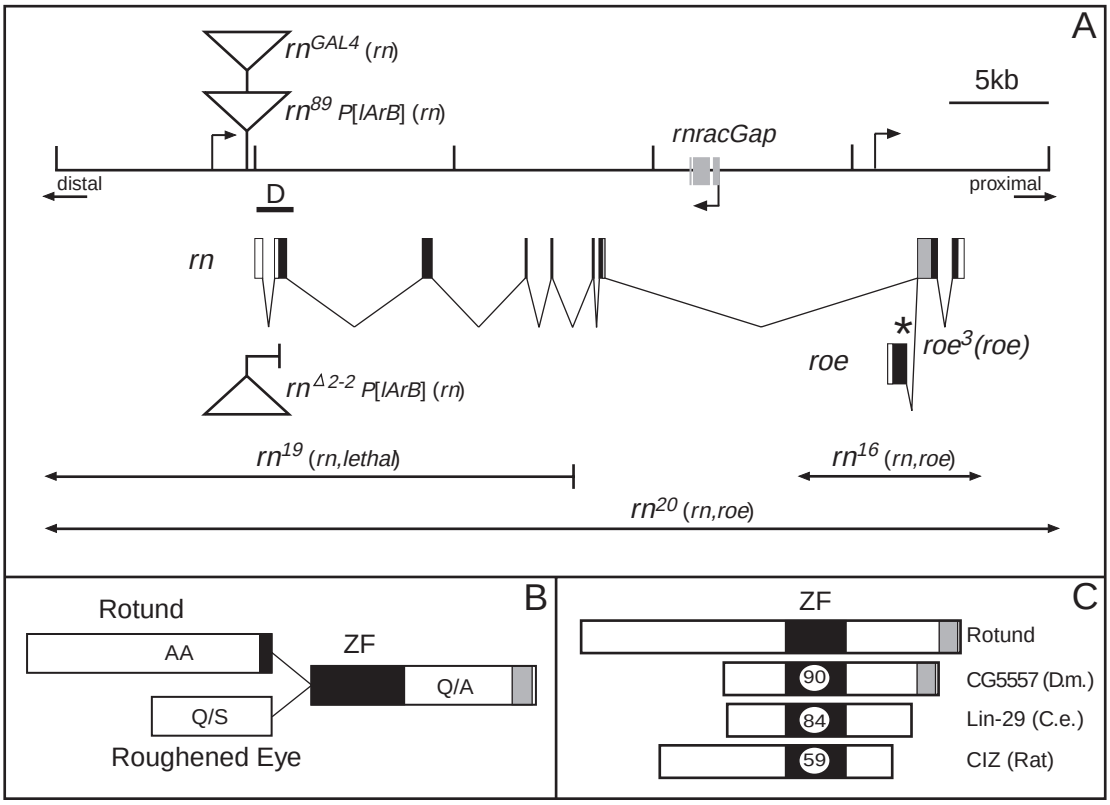

Fig. 1. (A) Genomic organization of the *rn* region. Insertion site of the three P elements is denoted by open triangles. The deletion in $rn^{\Delta 2-2}$ is denoted by the extended line. Fragment D was isolated in the previous study (Agnel et al., 1989) and used to initiate the screen for *rn*. Putative promoters are depicted as angled arrows. The *rn* and *roe* transcripts are outlined and the ORFs designated by black boxes for both genes. The ZF domain is represented by gray shading. Deletions used in this study are indicated at the bottom and breakpoints, where known, are shown. Data for rn^{19} and rn^{20} are based on previous studies (Agnel et al., 1989). rn^{16} was described as a smaller deletion mapping to the 3′ area (Agnel et al., 1989) but our work shows that it extends further, deleting both the common ZF coding exons and the *roe*-specific exons (not shown). The roe^3 mutation (asterisk), is a glutamine to an amber stop codon. (B) Predicted protein structure of Rn and Roe. The N-termini are unique but the C-termini, containing most of the ZF domain, are identical. The glutamine, serine and alanine stretches are designated Q, S and A, respectively. (C) Comparison of Rn with other ZF proteins. Rn has a few close homologs in *Drosophila* (D.m.), *C. elegans* (C.e.) and rat. Numbers in circles are the percentage of identical amino acids between Rn and the other proteins in the ZF domain. Rn, Roe and *Drosophila* CG5557 further share a C-terminal region of homology not present in the other proteins (gray).

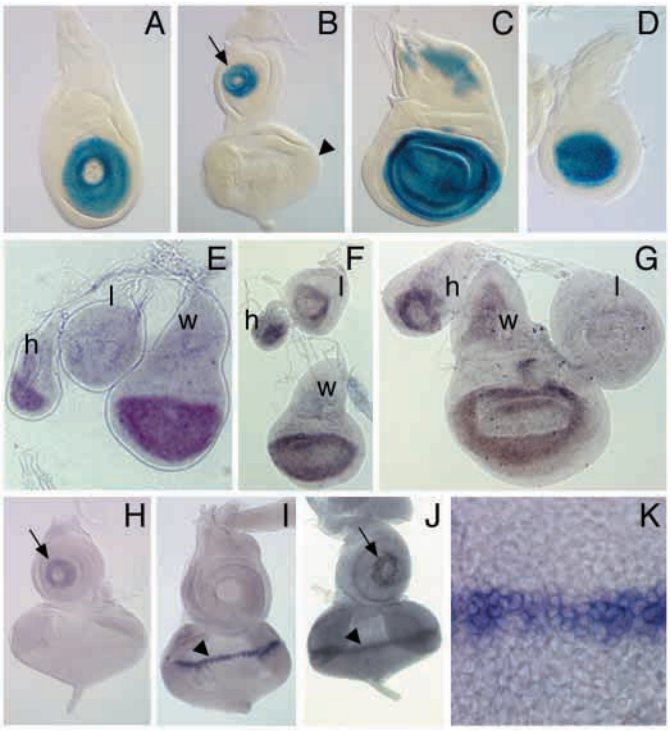

Fig. 2. Expression of *rn* and *roe* in third instar imaginal discs. (A-D) Late third instar rn^{89} imaginal discs stained with X-gal. Expression is seen as a wide ring in the leg disc (A) and the antennal portion of the eye-antenna disc (B, arrow). Note the lack of detectable expression in the eye portion (B, arrowhead). Expression is also evident in the central region and the notum of the wing disc (C) and in the central region of the haltere disc (D). (E-G) In situ hybridization to wild type using a *rn*-specific probe in early (E), mid (F), and late (G) third instar discs. Expression of *rn* is seen in a pattern similar to that of X-gal in rn^{89}. In the leg disc (l), the expression of *rn* is transient and evident only during 80-96 hours after egg laying. In contrast, the expression of *rn* in the wing (w) and haltere (h) is found throughout the third instar larval stages. (H-K) In situ hybridization of wild-type eye-antenna discs using *rn*-specific (H), *roe*-specific (I,K) and *rn/roe* common 3′ (J) probes. (H) Expression of *rn* is found only in the antennal portion (arrow), and (I) *roe* only in the eye portion of the eye-antennal disc (arrowhead). (J) Using the *rn/roe* common 3′ probe we detect the combined pattern of *rn* and *roe* and both the antennal (arrow) and the eye portion (arrowhead) show expression. (K) Expression of *roe* is found in a band of 4-6 cells at the morphogenetic furrow.

However, the fact that rn^{19} extends further distally, uncovering other complementation group(s), but does not produce *roe* phenotypes argues against eye-specific splicing of a long transcript originating from a promoter in the *rn* region. Instead, a more likely scenario would be the existence of an eye-specific promoter and exon(s). This notion was further supported by analysis of P-element insertions in the *rn* 5′ area that result in the *rn* phenotype and matching expression but not in the *roe* phenotype or eye disc expression (see below). These results prompted us to look for additional exons that could explain the molecular nature of the *roe* gene. By screening a larval cDNA library with a *rn* 3′ probe and by subsequent PCR analysis we isolated the *roe* cDNA. The *roe* gene utilizes the same two 3′ exons as *rn* but contains a different 5′ exon (Fig. 1A). As a result the predicted Roe protein shares the C-terminal region, including the ZF domain except the first finger, with Rn but differs in the N-terminal region (Fig. 1B). It is interesting to note that the *rn* genomic structure was not revealed by the analysis of the sequences carried out by the *Drosophila* Genome Project (Adams et al., 2000). Although parts of the *rn* coding regions were identified (CG14600, CG14601, CG14603 and CG10040), the *rn* transcript was not predicted, probably because *rn* has several small exons spread over 50 kb. In contrast, the *roe* transcript was accurately predicted, short of one aa error in the splice junction between exons 1 and 2 (CG10040). At the submission of this study, the *rn* and *roe* cDNAs had not been isolated in the BDGP or RIKEN expressed sequence tag (EST) projects.

Molecular analysis of *rotund* and *roughened eye* mutations

The genomic structure of the *rn* locus that we propose fits well both with previous studies as well as with our molecular analysis of *rn* and *roe* alleles. First, rn^{16} and rn^{20} are deletions that show both *rn* and *roe* phenotypes, while the rn^{19} deletion only shows *rn* phenotypes (Agnel et al., 1989). In agreement, rn^{16} deletes both the common ZF coding exons and *roe*-specific exons, rn^{20} deletes the whole region, and rn^{19} removes most of the *rn*-specific exons (Fig. 1A). Second, we sequenced roe^{3}, a strong *roe*-specific allele, and show that it is the result of a nonsense mutation in the *roe*-specific exon. This mutation does not affect the common 3′ exons and explains why roe^{3} acts as a *roe* null allele but does not show *rn* phenotypes. Third, rn^{89}, a *lacZ*-containing P-element transposon allele (Couso and Bishop, 1998) was shown to be inserted within the 5′ region of the *rn* gene. This explains why it only displays *rn* and not *roe* phenotypes. In addition, imprecise excision of rn^{89} yielded $rn^{\Delta 2-2}$, which contains a deletion of the first and part of the second *rn* exon (Fig. 1A). As expected, $rn^{\Delta 2-2}$ displays a *rn* null phenotype (Fig. 3C,I) but no eye phenotype. In agreement with this, in situ hybridization failed to detect any *rn* transcript in $rn^{\Delta 2-2}$ mutant discs (not shown). We further generated $rn^{GAL4\#5}$ by P-element conversion of rn^{89}. $rn^{GAL4\#5}$ displays a stronger leg phenotype than rn^{89}, possibly due to differences in the structure of the P element, but again no aberrant eye phenotype (not shown). Wild-type revertants of rn^{89} and $rn^{GAL4\#5}$ were generated that complement other *rn* alleles, verifying that in both cases the *rn* phenotype was caused by the P-element insertion.

Expression of *rotund* and *roughened eye*

We detect expression of *rn* and *roe* in developing imaginal discs, as well as in the embryonic and larval CNS. Here we will focus on the expression in the imaginal discs. Expression of *rn* commences during the early third larval instar in the leg, wing, haltere and antennal part of the eye-antennal imaginal disc (Fig. 2E-H). Expression of *rn* is observed as a ring in the leg and antenna discs and in the presumptive wing pouch and capitellum of wing and haltere discs respectively. In late third instar, expression of *rn* in the leg disc is no longer evident, but is maintained in the other discs (Fig. 2G). We also studied the expression of *lacZ* in both rn^{89} and in $rn^{GAL4\#5}$/*UAS-lacZ* larvae to determine *rn* expression. In both genotypes, expression of *lacZ* is in agreement with the *rn* in situ hybridization, except for the persistence of tarsal expression (Fig. 2A-D), but in neither line do we detect expression in the eye disc. Expression of *roe* commences in the third instar and

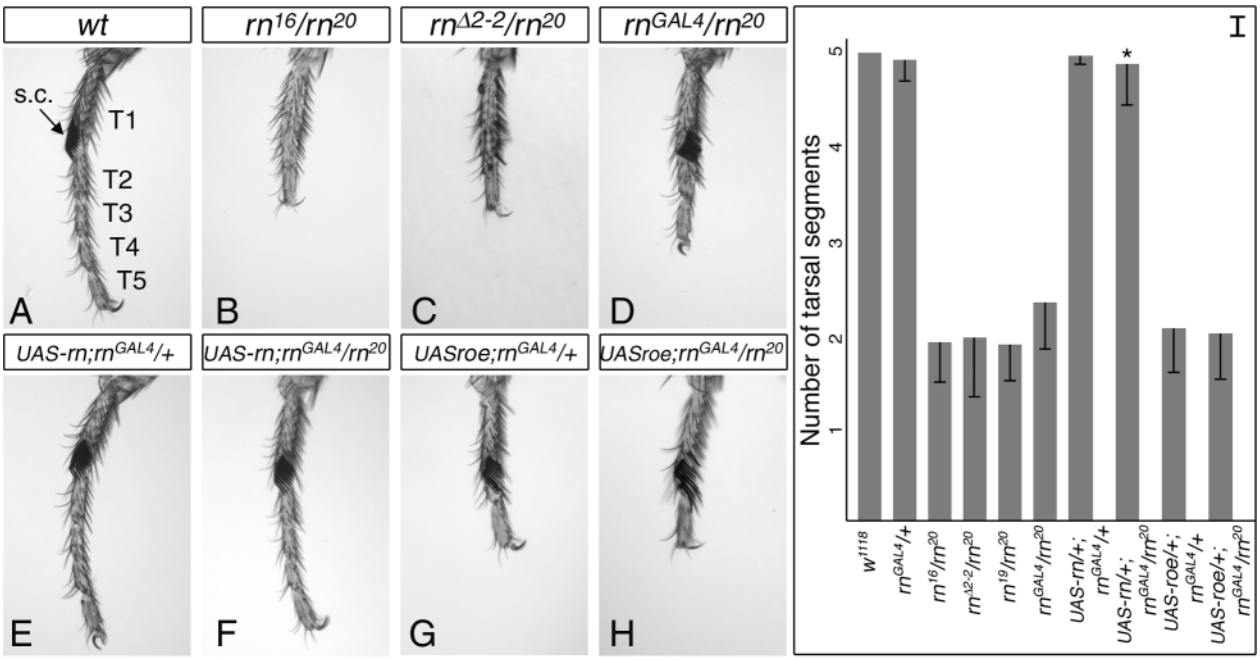

Fig. 3. Rescue of the *rn* leg phenotype. (A-H) Adult male forelegs and (I) quantification of the number of tarsal segments. (A) Wild-type leg with sex comb (s.c.), 5 distinct tarsal segments (T1-5), and a claw at the tip of the 5th tarsus. (B) rn^{16}/rn^{20}, a genetic null. The sex comb is completely missing in all cases and the five tarsi appear fused into one segment. Note, however, that the claw is still present. (C) $rn^{\Delta 2-2}/rn^{20}$, which acts as a genetic null. (D) $rn^{GAL4\#5}/rn^{20}$, a hypomorphic allelic combination. The sex comb is present and appears normal. The claw is normal. However, the tarsi are fused into two to three tarsal-like segments. (E) *UAS-rn /+;*$rn^{GAL4\#5}$*/+*. *UAS-rn* causes no obvious disruption of the leg. (F) Rescue of *rn* mutants in *UAS-rn /+;*$rn^{GAL4\#5}/rn^{20}$. The *rn* cDNA, expressed using the *GAL4/UAS* system, rescues the leg phenotype. (G) *UAS-roe/+;*$rn^{GAL4\#5}$*/+*. *UAS-roe* has negative effects when expressed in the *rn* pattern. (H) *UAS-roe/+;*$rn^{GAL4\#5}/rn^{20}$. *UAS-roe* is unable to rescue *rn* mutants. (I) Quantification of tarsi in wild type, *rn* mutants and rescue flies. The apparent number of tarsal segments was determined in *rn* mutants and rescue flies (>20 flies and >120 legs/genotype). The rescue is statistically significant to $P<0.001$ using a two-tailed *t*-test. Error bars represent the standard deviation. Temperature for rescue is 18°C though similar results were observed at 22°C (not shown).

is confined to the eye part of the eye-antennal imaginal disc in a band of 4-6 cells at the morphogenetic furrow (Fig. 2I,K). We find no evidence of *roe* expression in other imaginal discs.

The expression of *rn* and *roe* is in agreement with the observed phenotypes. For instance, *rn* mutants have defects in wings and halteres, and correspondingly *rn* is expressed in the appropriate presumptive regions in wing and haltere imaginal discs. In the leg, *rn* mutants display fusion of all 5 leg tarsi into one fused tarsal-like segment. In agreement with this, *rn* is expressed in a sub-distal ring that represents the presumptive tarsus, as revealed by the persistent tarsal expression of *rn*-driven *lacZ* in late third instar discs. Similarly, *roe* specifically affects the eye, and mutants have rough eyes and reduced numbers of photoreceptors (Ma et al., 1996). Accordingly, we observe expression of *roe* in the eye part of the eye-antennal imaginal disc but not in other imaginal discs. The mutually exclusive patterns of expression of *rn* and *roe* raised the issue of whether they may in fact negatively regulate each other. To determine this, we analyzed the expression of *roe* in *rn* mutant imaginal discs and conversely the expression of *rn* in *roe* mutant imaginal discs. These studies revealed no apparent changes in the expression of *rn* and *roe* when compared to wild type, indicating that there is no cross-regulation between *rn* and *roe* (not shown).

Rescue of *rotund*

Owing to the complexity of the *rn* locus we wanted to further verify the authenticity of our *rn* and *roe* cDNAs by rescue experiments. For the *rn* rescue we focused on the leg phenotype and used the $rn^{GAL4\#5}$ line that shows strong leg phenotypes over rn^{20} (Fig. 3A,D,I). By providing *rn* function with *UAS-rn*, we observe rescue of the $rn^{GAL4\#5}/rn^{20}$ leg phenotypes, often to a level indistinguishable from the wild-type leg (Fig. 3F,I, $P<0.001$). We do not observe any dominant effect in the leg of *UAS-rn* in a heterozygous background (Fig. 3E,I).

The structure of the *rn* genomic region and the differential expression in imaginal discs explains why *rn* and *roe* can be genetically separated and affect different tissues. However, the *rn* and *roe* gene products are also different, and the first ZF is truncated in the Roe protein (Fig. 1B), intriguing given that the first finger of Krüppel-type ZF proteins has been shown to be involved in DNA-binding (Avram et al., 1999; Hamilton et al., 1998). Rn and Roe further differ in the N-terminal regions where they contain stretches of glutamine/serine (Roe) or alanine (Rn), often found in transcriptional activator and repressor domains respectively (Gerber et al., 1994; Lanz et al., 1995; Licht et al., 1994; Madden et al., 1993; Nowling et al., 2000). This raised the possibility that these two proteins may have different activities and may not be interchangeable. To address this issue we misexpressed *roe* in the leg disc and also attempted to rescue *rn* with *roe*. When *roe* is misexpressed in the developing leg disc using $rn^{GAL4\#5}$, we noticed a negative effect with reduced number of tarsi, similar to *rn* mutants (Fig.

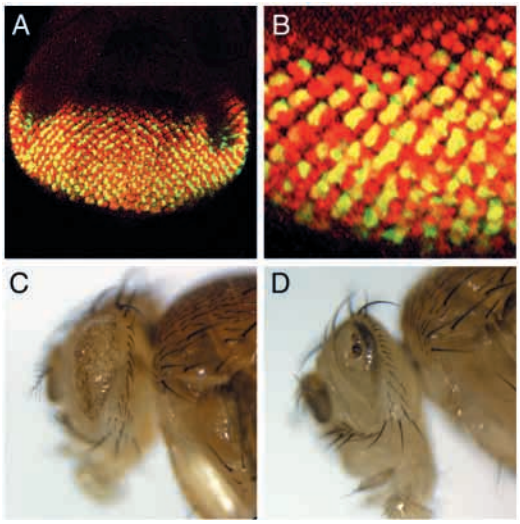

Fig. 4. (A,B) Expression of *sev-GAL4*, visualized by crossing to *UAS-lacZ* and staining for anti-β-gal (green), in relation to Elav (red) expression. Expression of *sev-GAL4* commences posterior to the morphogenetic furrow in subsets of photoreceptors, as evident by the overlap with Elav. In addition, *sev-GAL4* expression is observed in cells adjacent to the developing photoreceptors, most likely corresponding to mystery and cone cells. (C,D) Misexpression of *rn* (C) in *UAS-rn/+;GMR-GAL4/+* and *roe* (D) *UAS-roe/+;GMR-GAL4/+* both lead to disruptions in the morphology and size of the adult eye. These include an apparent loss of pigment cells and bristle cells, as well as the presence of patches of necrotic tissue (black).

3G,I). Furthermore, in a *rn* mutant background ($rn^{GAL4\#5}/rn^{20}$) we observe no evidence of rescue by *UAS-roe* (Fig. 3H,I).

Rescue of roughened eye

We also wanted to rescue *roe* mutants using the *GAL4/UAS* system. The *roe* rescue was complicated by the fact that we did not have a *GAL4* insertion in the *roe* gene. This is especially relevant given the dynamic pattern of *roe* expression in the eye disc, with transient expression in a band of approx. 4-6 cells at the morphogenetic furrow (Fig. 2I,K). We were unable to identify a *GAL4* line that would express precisely in the *roe* pattern and instead attempted to rescue *roe* using *GAL4* drivers that would drive in photoreceptors. To this end, we tested several eye disc *GAL4* driver lines for ectopic effects. Not surprisingly, strong pan-eye drivers such as *GMR-GAL4* lead to dramatic phenotypes with loss of pigment and bristle cells (Fig. 4D). A novel *sevenless-GAL4* (*sev-GAL4*) line that expresses *GAL4* in the photoreceptors, cone and mystery cells (Fig. 4A,B) showed little if any sign of rough eye morphology when crossed to *UAS-roe* (not shown). Using *sev-GAL4* crossed to *UAS-roe* in a *roe* null mutant background (rn^{16}/rn^{20}) we observe partial rescue of the eye phenotypes with increased eye size and reduced roughness (Fig. 5A-C). To quantify the *roe* rescue we counted the number of adult R1-7 photoreceptors in wild-type, mutant and rescued flies. These results confirm previous studies (Ma et al., 1996) and show that *roe* mutants have a reduced number of photoreceptors compared to wild type (Fig. 5E). In line with the apparent morphological rescue we find significantly increased numbers of photoreceptors in rescued flies when compared to mutants ($P<0.04$, Fig. 5E). Given that we were unable to use a *GAL4* driver line that perfectly matched the dynamic expression of *roe* in eye discs, we believe that this partial rescue supports the proposed identity of the *roe* gene. As in the *rn* rescue experiments, we wanted to address whether *rn* is interchangeable with *roe* and could provide rescue activity in the eye. First we tested the activity of *UAS-rn* in the eye by misexpressing it using *GMR-GAL4* and *sev-GAL4*. This leads to severe rough eye phenotypes with *GMR-GAL4* (Fig. 4C) and little if any sign of rough eye morphology with *sev-GAL4* (not shown). In a *roe* null mutant background (rn^{16}/rn^{20}) we find no evidence of rescue by adding *UAS-rn* (Fig. 5B-E).

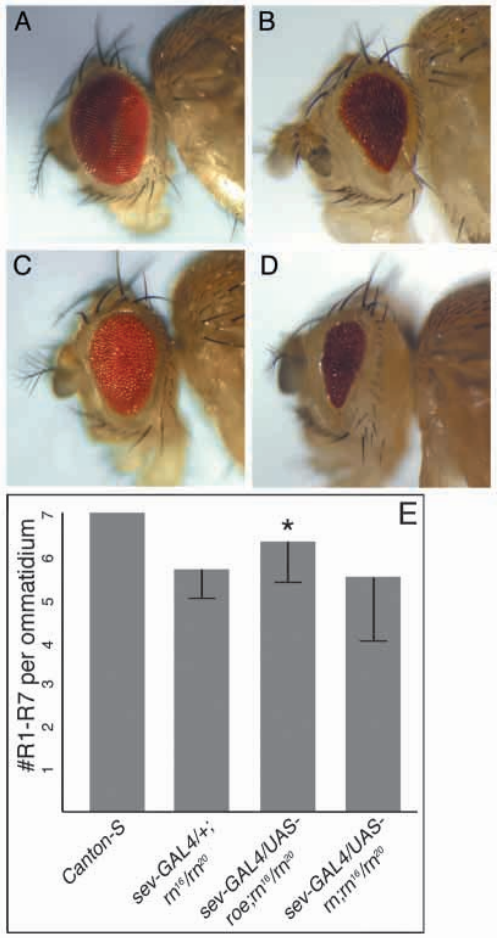

Fig. 5. Rescue of *roe*. (A-D) Adult eyes and (E) quantification of photoreceptors. (A) Wild type. (B) rn^{16}/rn^{20} a *roe* null combination displays a small and rough eye. (C) *UAS-roe* can rescue *roe*. *sev-GAL4/UAS-roe;*rn^{16}/rn^{20} have larger and apparently less rough eyes than *roe*. (D) *UAS-rn* fails to rescue *roe*. *sev-GAL4/UAS-rn;*rn^{16}/rn^{20} eye shows no sign of rescue, instead an apparent enhancement of the *roe* phenotype. (E) Quantification of the rescue of *roe* mutants. Adult eyes were sectioned and the number of Elav-positive cells in each ommatidia was counted. Wild-type ommatidia carry the typical seven (R1-7) photoreceptors (the R8 photoreceptor cell body is located slightly offset and was not included). In *roe* mutants we find an average of 5.7 photoreceptors, which is rescued to 6.3 by providing *roe* activity using *UAS-roe* ($P<0.04$). Using *UAS-rn* we find no evidence of rescue and *roe* ommatidia contain an average of 5.6 photoreceptors per ommatidia. In addition we find ommatidia with 4 or sometimes only 3 photoreceptors, something not observed in the other genotypes, indicating a negative action of *UAS-rn*.

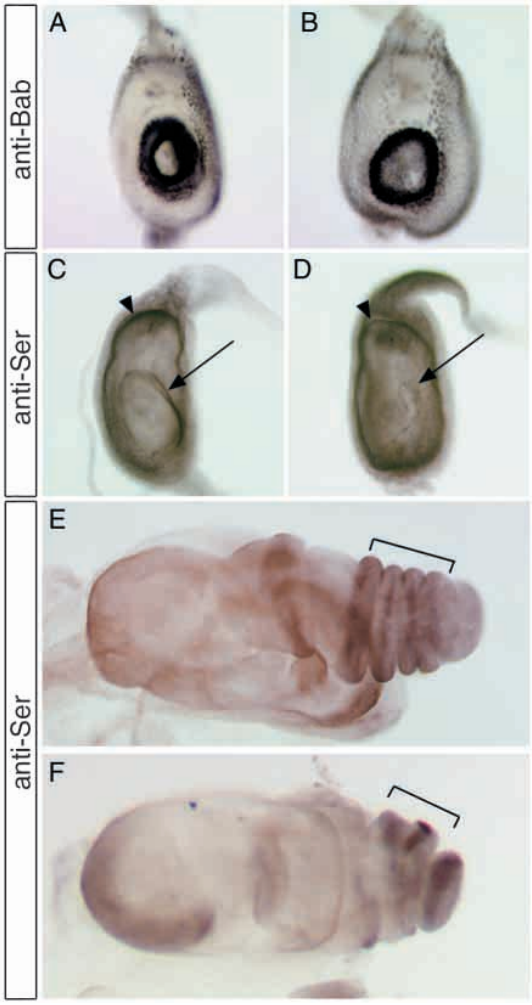

Fig. 6. (A-D) Mid third instar larval and (E,F) pupal leg imaginal discs. Expression of Bab in wild-type (A) and rn^{16}/rn^{20} (B) leg discs show that neither the pattern nor the intensity of Bab staining is affected in *rn*. Expression of Ser in wild type (C,E) and rn^{16}/rn^{20} (D,F). In wild-type leg discs (C) Ser expression is observed as a ring in the first tarsal fold (arrow) and in the proximal furrow (arrowhead). In rn^{16}/rn^{20} leg discs (D) Ser expression is down-regulated in the tarsal fold (arrow) but maintained in the proximal furrow (arrowhead). Similarly, in pupal leg discs Ser appears to be down-regulated in the presumptive tarsal area where *rn* is normally expressed. Compare bracketed areas in (E) wild type and in (F) rn^{16}/rn^{20}.

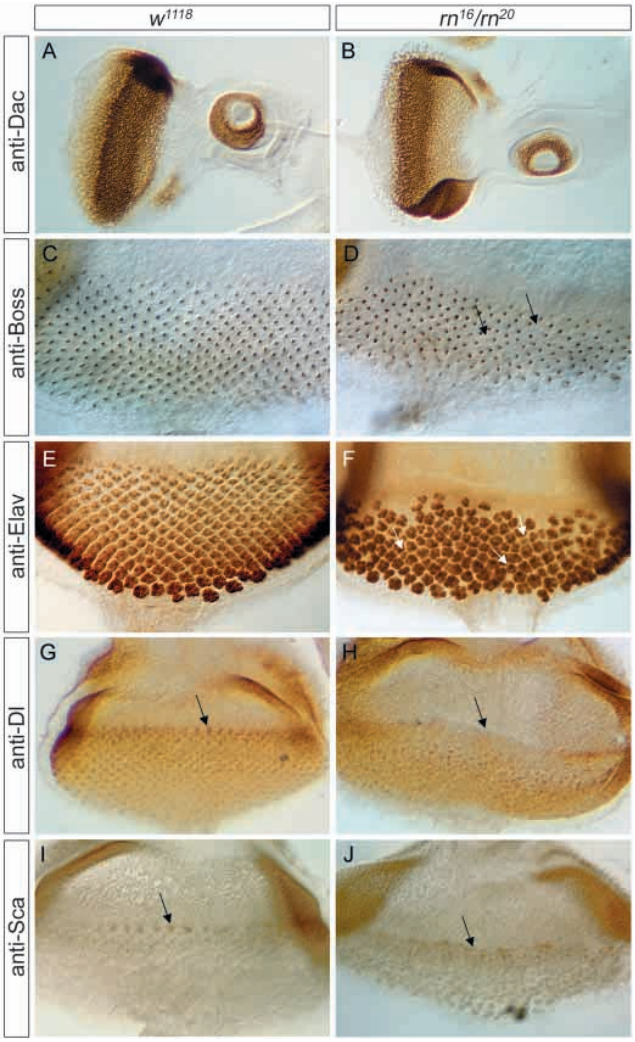

Fig. 7. Third instar larval eye-antennal discs. (A,C,E,G) Wild-type discs, and (B,D,F,H) rn^{16}/rn^{20} discs. Expression of Dac in wild type (A) and *roe* mutant (B) shows that Dac expression is unaffected and that general eye disc patterning appears normal. Dac further appears unchanged in the antennal spot. Expression of Boss (C,D) and Elav (E,F) reveals that the highly ordered array of developing photoreceptors observed in wild type (C,E) is affected in *roe* (D,F). Boss expression is apparently absent from some developing photoreceptor clusters (arrows in D), and Elav expression reveals clusters with reduced number of photoreceptors (arrows in F). (G,H) Expression of Dl. In wild type (G) Dl expression is observed in clusters at the morphogenetic furrow (arrow) and in subsets of cells posterior to it. In *roe* (H) the punctate expression of Dl at the furrow is affected and only present as a diffuse band (arrow). Posterior to the furrow, Dl expression is disorganized (H). Expression of Sca in wild type (I) and *roe* (J) is similar to Dl.

Molecular context for *rotund* and *roughened eye* activity

Previous studies suggested that *rn* and *roe* act late during development of their respective tissues, perhaps during terminal differentiation (Godt et al., 1993; Renfranz and Benzer, 1989). To further explore the function of *rn* and *roe* during leg and eye development, we have examined the expression of genes that play key roles during development of these tissues. We first studied the leg disc and analyzed genes whose expression abuts or overlaps that of *rn*. Dachshund (Dac), a nuclear factor required for normal leg development, is expressed at early stages of leg development in a ring pattern that abuts the early *rn*-expressing ring (M. I. G., S. A. Bishop and J. P. C., unpublished). Bric a brac (Bab), a BTB-domain containing transcription factor, has been suggested to be active late in limb development and is expressed in a similar pattern to *rn* in the leg (Godt et al., 1993). Furthermore, *bab* mutants show similar (though not identical) phenotypes to *rn* mutants in the tarsal segments of the leg (Godt et al., 1993). Interestingly, neither Dac nor Bab appears to be regulated by *rn* as revealed by staining of third instar leg discs (Fig. 6A,B; not shown). These results suggest that *rn* might act in parallel to, or downstream of, *dac* and *bab* to specify tarsal segment

identity. Ser, a ligand for the Notch (N) receptor, is expressed in presumptive joint areas in larvae and pupa leg discs and controls the development of the leg joints (Bishop et al., 1999). In wild-type mid-third instar leg discs, Ser is expressed in the first tarsal fold, which coincides with the *rn*-expressing ring. In *rn*, Ser is down-regulated in the tarsal ring but not outside it (Fig. 6C,D). In pupal leg discs, Ser expression, normally present in four stripes within the presumptive tarsal area (Fig. 6E), is present in fewer and less defined stripes in *rn* (Fig. 6F).

The *roe* rough eye phenotype is reflected in reduced numbers of photoreceptors present in adult ommatidia (Brand and Campos-Ortega, 1990) (this study). To determine whether *roe* mutants show early patterning defects in the eye-antennal disc, we analyzed expression of Dac, which plays an early role in the eye disc and is expressed in a broad domain spanning both sides of the morphogenetic furrow (MF) (Mardon et al., 1994). Since *dac* mutants have a more severe eye phenotype than *roe* we anticipated that Dac would not be regulated by *roe*, and as expected we observe no change in the pattern of Dac staining in *roe* when compared to wild type (Fig. 7A,B). Next we analyzed third instar eye-antennal discs with antibodies to Elav and to Bride of Sevenless (Boss), a marker of R8 photoreceptors (Hart et al., 1990). In wild-type eye discs, Elav and Boss are expressed in a stereotyped pattern immediately posterior to the MF (Fig. 7C,E). In *roe* mutants, expression of Elav and Boss reveals abnormal photoreceptor differentiation with apparent gaps in the expression of both markers posterior to the MF (Fig. 7D,F). Elav expression also indicates that photoreceptor clusters frequently have fewer photoreceptors than normal (Fig. 7E,F). Expression of Elav and Boss further reveals an apparent failure of the MF to progress in a straight line from dorsal to ventral. The MF appears to progress more slowly in some areas, creating a wave-like appearance of developing photoreceptor clusters near the MF (Fig. 7C-F). These results indicate that *roe* function is centered around the MF, a notion that fits well with the strong but transient *roe* expression seen at the MF (Fig. 2I,K). We therefore analyzed markers expressed at the MF, and since *roe* has been shown to interact genetically with the N^{Spl} mutation (Brand and Campos-Ortega, 1990), we examined expression of Delta (Dl), a N ligand (Vassin et al., 1987), and Scabrous (Sca), a secreted glycoprotein implicated in N signaling (Baker et al., 1990). In wild type, Dl and Sca are expressed in clusters of cells at the MF, and expression is maintained posterior to the MF in subsets of cells (Fig. 7G,I). In *roe* mutants, the punctate expression of Dl and Sca is lost at the MF and replaced by a diffuse band of expression. Posterior to the MF, expression is punctate but appears disorganized (Fig. 7H,J).

DISCUSSION

The *rn* and *roe* loci are tightly linked and this study reveals the underlying molecular basis for this linkage. Intriguingly, our work shows that *roe* is part of the *rn* gene and is represented by a related but distinct transcript. The rescue and misexpression experiments support the notion that *rn* and *roe* play different roles during imaginal disc development not only because of their differential expression but also because of distinct activities of the Rn and Roe proteins. These activities could involve different target DNA sequences and/or different transcriptional effects, perhaps based on their different ZF and glutamine/alanine/serine stretches.

Regarding the function of the *rnracGAP*, both our work and previous studies argue against any involvement of *rnracGAP* in the *rn* or *roe* phenotypes (Agnel et al., 1989; Agnel et al., 1992a; Hoemann et al., 1996). In situ studies indicate that *rnracGAP* is only expressed at low levels in the imaginal discs during pupal stages (Agnel et al., 1989; Agnel et al., 1992a; Hoemann et al., 1996). In addition, there is no obvious difference in the severity of *rn* and *roe* phenotypes whether or not the *rnracGAP* is simultaneously removed. For instance, we have found no significant difference in the severity of *rn* leg phenotypes in rn^{20}/rn^{20} (that removes *rn*, *roe* and *rnracGAP*) compared to rn^{19}/rn^{20} (rn^{19} does not remove *rnracGAP*). Similarly, roe^{3}/rn^{20} (roe^{3} has a premature stop codon in the *roe*-specific exon) displays as severe of an eye phenotype as rn^{20}/rn^{20} (not shown). Furthermore, we can rescue *rn* and *roe* mutants with the *rn* and *roe* cDNAs. Recent studies may indicate an involvement of *rnracGAP* specifically in male fertility, and high levels of *rnracGAP* expression have been observed in the adult testis (Agnel et al., 1989; Agnel et al., 1992a; Hoemann et al., 1996). The rn^{89} and $rn^{GAL4\#5}$ P-element insertions described here may provide useful starting materials for the generation of mutations specifically affecting the *rnracGAP* by local P-element mobilization.

Little is known about the genetic cascades within which *roe* and *rn* are acting. The results from eye-antennal imaginal discs indicate that *roe* acts at the morphogenetic furrow, as evident both from its expression and from the effects on Dl and Sca expression in *roe* mutants. Both *Dl* and *sca* play roles in spacing the array of ommatidial preclusters in the morphogenetic furrow (Baker et al., 1990; Baker and Zitron, 1995; Ellis et al., 1994), and it is interesting to note that the expression of *roe* at the furrow is not evenly distributed and appears stronger in clusters of cells (Fig. 2I). Genetic screens for modifiers of the N^{spl} mutation identified *roe* as an enhancer, and *sca* and *Dl* as suppressors of the N^{spl} eye phenotype (Brand and Campos-Ortega, 1990). Given the dynamics of N signaling, these results support models where Roe acts to either positively or negatively regulate Dl and Sca. A genetic interaction screen for enhancers of *glass* also identified *roe* (Ma et al., 1996), an interesting finding given that ectopic expression of *roe* using *GMR-GAL4* leads to a *glass*-like phenotype with a loss of bristles and pigment cells (Fig. 4E,F).

In the leg, *rn* expression is the earliest marker known for tarsal development (Couso and Bishop, 1998). *rn* is required for the development of this region and for its subsequent patterning, as observed by the loss of Ser expression. Thus, the transient expression of *rn* in the leg might reveal that the intercalation of the presumptive tarsal region between the distal tip and medial leg regions occurs during early third instar.

It is increasingly common, even in invertebrates, to find genes that utilize two or more promoters (Gower et al., 2001; Krishnan et al., 1995; Li et al., 1999; Mevel-Ninio et al., 1995). Although this may lead to the generation of different proteins, it is often unclear whether the proteins have distinct activities. In fact, this issue is not easily resolved by traditional forward genetics and subsequent molecular analysis, since even if a locus can be genetically dissected into different subfunctions, this does not identify whether the different proteins have distinct activities. Perhaps the best way to test whether the variant proteins are

interchangeable in vivo, is by cross-rescue in each others domain of expression. The *rn* gene is a clear example of a locus that utilizes both tissue-specific promoters and functionally distinct proteins to achieve functional diversity, a scenario likely to be observed more and more frequently in the post-genomic era.

We thank J. B. Thomas and P. H. Taghert for advice. We thank A. Bailey and G. M. Rubin for the *sev-GAL4* lines, and R. Griffin-Shea for sharing fly lines and DNAs. G. Gloor provided advice on P-element conversion. We thank L. Zipursky, K. Irvine and E. Knust for antibodies. We are grateful to The Bloomington Stock Center for providing fly lines. We thank N. Perrimon, A. Michelson and A. Simcox for critically reading the manuscript. B. Borsari provided excellent technical assistance. This work was supported by grants from NIH (RO1 NS39875-01, T32MH20017) to S. T. and S. E. S. and by The Wellcome Trust (Senior Research Fellowship and supplementary Grant) to J. P. C. and M. I. G.

REFERENCES

Adams, M. D., Celniker, S. E., Holt, R. A., Evans, C. A., Gocayne, J. D., Amanatides, P. G., Scherer, S. E., Li, P. W., Hoskins, R. A., Galle, R. F. et al. (2000). The genome sequence of Drosophila melanogaster. *Science* **287**, 2185-2195.

Agnel, M., Kerridge, S., Vola, C. and Griffin-Shea, R. (1989). Two transcripts from the rotund region of Drosophila show similar positional specificities in imaginal disc tissues. *Genes Dev.* **3**, 85-95.

Agnel, M., Roder, L., Griffin-Shea, R. and Vola, C. (1992a). The spatial expession of Drosophila rotund gene reveals that the imaginal discs are organized in domains along the proximal-distal axis. *Roux's Arch. Dev. Biol.* **201**, 284-295.

Agnel, M., Roder, L., Vola, C. and Griffin-Shea, R. (1992b). A Drosophila rotund transcript expressed during spermatogenesis and imaginal disc morphogenesis encodes a protein which is similar to human Rac GTPase-activating (racGAP) proteins. *Mol. Cell Biol.* **12**, 5111-5122.

Avram, D., Leid, M. and Bakalinsky, A. T. (1999). Fzf1p of Saccharomyces cerevisiae is a positive regulator of SSU1 transcription and its first zinc finger region is required for DNA binding. *Yeast* **15**, 473-480.

Baker, N. E., Mlodzik, M. and Rubin, G. M. (1990). Spacing differentiation in the developing Drosophila eye: a fibrinogen-related lateral inhibitor encoded by scabrous. *Science* **250**, 1370-1377.

Baker, N. E. and Zitron, A. E. (1995). Drosophila eye development: Notch and Delta amplify a neurogenic pattern conferred on the morphogenetic furrow by scabrous. *Mech. Dev.* **49**, 173-189.

Bishop, S. A., Klein, T., Arias, A. M. and Couso, J. P. (1999). Composite signalling from Serrate and Delta establishes leg segments in Drosophila through Notch. *Development* **126**, 2993-3003.

Brand, A. H. and Perrimon, N. (1993). Targeted gene expression as a means of altering cell fates and generating dominant phenotypes. *Development* **118**, 401-415.

Brand, M. and Campos-Ortega, J. A. (1990). Second-site modifiers of the split mutation of Notch define genes involved in neurogenesis in Drosophila melanogaster. *Roux's Arch. Dev. Biol.* **198**, 275-285.

Cavener, D. R., Otteson, D. C. and Kaufman, T. C. (1986). A rehabilitation of the genetic map of the 84B-D region in Drosophila melanogaster. *Genetics* **114**, 111-123.

Cavener, D. R. and Ray, S. C. (1991). Eukaryotic start and stop translation sites. *Nucleic Acids Res.* **19**, 3185-3192.

Couso, J. P. and Bishop, S. A. (1998). Proximodistal development in the legs of Drosophila. *Int. J. Dev. Biol.* **42**, 345-352.

Ellis, M. C., Weber, U., Wiersdorff, V. and Mlodzik, M. (1994). Confrontation of scabrous expressing and non-expressing cells is essential for normal ommatidial spacing in the Drosophila eye. *Development* **120**, 1959-1969.

Gerber, H. P., Seipel, K., Georgiev, O., Hofferer, M., Hug, M., Rusconi, S. and Schaffner, W. (1994). Transcriptional activation modulated by homopolymeric glutamine and proline stretches. *Science* **263**, 808-811.

Godt, D., Couderc, J. L., Cramton, S. E. and Laski, F. A. (1993). Pattern formation in the limbs of Drosophila: bric a brac is expressed in both a gradient and a wave-like pattern and is required for specification and proper segmentation of the tarsus. *Development* **119**, 799-812.

Gower, N. J., Temple, G. R., Schein, J. E., Marra, M., Walker, D. S. and Baylis, H. A. (2001). Dissection of the promoter region of the inositol 1,4,5-trisphosphate receptor gene, itr-1, in C. elegans: a molecular basis for cell-specific expression of IP3R isoforms. *J. Mol. Biol.* **306**, 145-157.

Hamilton, T. B., Borel, F. and Romaniuk, P. J. (1998). Comparison of the DNA binding characteristics of the related zinc finger proteins WT1 and EGR1. *Biochemistry* **37**, 2051-2058.

Hart, A. C., Kramer, H., Van Vactor, D. L., Jr., Paidhungat, M. and Zipursky, S. L. (1990). Induction of cell fate in the Drosophila retina: the bride of sevenless protein is predicted to contain a large extracellular domain and seven transmembrane segments. *Genes Dev.* **4**, 1835-1847.

Hay, B. A., Maile, R. and Rubin, G. M. (1997). P element insertion-dependent gene activation in the Drosophila eye. *Proc. Natl. Acad. Sci. USA* **94**, 5195-5200.

Hoemann, C. D., Bergeret, E., Guichard, A. and Griffin-Shea, R. (1996). Alternative splicing of the Drosophila melanogaster rotundRacGAP gene. *Gene* **168**, 135-141.

Kerridge, S. and Thomas-Cavallin, M. (1988). Appendage morphogenesis in Drosophila: a developmental study of the rotund (rn) gene. *Roux's Arch. Dev. Biol.* **197**, 19-26.

Krishnan, S. N., Frei, E., Schalet, A. P. and Wyman, R. J. (1995). Molecular basis of intracistronic complementation in the Passover locus of Drosophila. *Proc. Natl. Acad. Sci. USA* **92**, 2021-2025.

Lanz, R. B., Wieland, S., Hug, M. and Rusconi, S. (1995). A transcriptional repressor obtained by alternative translation of a trinucleotide repeat. *Nucleic Acids Res.* **23**, 138-145.

Li, W., Streit, A., Robertson, B. and Wood, W. B. (1999). Evidence for multiple promoter elements orchestrating male-specific regulation of the her-1 gene in Caenorhabditis elegans. *Genetics* **152**, 237-248.

Licht, J. D., Hanna-Rose, W., Reddy, J. C., English, M. A., Ro, M., Grossel, M., Shaknovich, R. and Hansen, U. (1994). Mapping and mutagenesis of the amino-terminal transcriptional repression domain of the Drosophila Kruppel protein. *Mol. Cell Biol.* **14**, 4057-4066.

Ma, C., Liu, H., Zhou, Y. and Moses, K. (1996). Identification and characterization of autosomal genes that interact with glass in the developing Drosophila eye. *Genetics* **142**, 1199-1213.

Madden, S. L., Cook, D. M. and Rauscher, F. J., 3rd. (1993). A structure-function analysis of transcriptional repression mediated by the WT1, Wilms' tumor suppressor protein. *Oncogene* **8**, 1713-1720.

Mardon, G., Solomon, N. M. and Rubin, G. M. (1994). *dachshund* encodes a nuclear protein required for normal eye and leg development in *Drosophila*. *Development* **120**, 3473-3486.

Mevel-Ninio, M., Terracol, R., Salles, C., Vincent, A. and Payre, F. (1995). ovo, a Drosophila gene required for ovarian development, is specifically expressed in the germline and shares most of its coding sequences with shavenbaby, a gene involved in embryo patterning. *Mech. Dev.* **49**, 83-95.

Nakamoto, T., Yamagata, T., Sakai, R., Ogawa, S., Honda, H., Ueno, H., Hirano, N., Yazaki, Y. and Hirai, H. (2000). CIZ, a zinc finger protein that interacts with p130(cas) and activates the expression of matrix metalloproteinases. *Mol. Cell Biol.* **20**, 1649-1658.

Nowling, T. K., Johnson, L. R., Wiebe, M. S. and Rizzino, A. (2000). Identification of the transactivation domain of the transcription factor Sox-2 and an associated co-activator. *J. Biol. Chem.* **275**, 3810-3818.

O'Neill, E. M., Rebay, I., Tjian, R. and Rubin, G. M. (1994). The activities of two Ets-related transcription factors required for Drosophila eye development are modulated by the Ras/MAPK pathway. *Cell* **78**, 137-147.

Renfranz, P. J. and Benzer, S. (1989). Monoclonal antibody probes discriminate early and late mutant defects in development of the Drosophila retina. *Dev. Biol.* **136**, 411-429.

Rougvie, A. E. and Ambros, V. (1995). The heterochronic gene lin-29 encodes a zinc finger protein that controls a terminal differentiation event in *Caenorhabditis elegans*. *Development* **121**, 2491-2500.

Sepp, K. J. and Auld, V. J. (1999). Conversion of lacZ enhancer trap lines to GAL4 lines using targeted transposition in Drosophila melanogaster. *Genetics* **151**, 1093-1101.

Spradling, A. C. and Rubin, G. M. (1982). Transposition of cloned P-elements into *Drosophila* germ line chromosomes. *Science* **218**, 341-347.

Tautz, D. and Pfeile, C. (1989). A non-radioactive in situ hybridization method for the localization of specific RNAs in Drosophila embryos reveals translational control of the segmentation gene *hunchback*. *Chromosoma* **98**, 81-85.

Vassin, H., Bremer, K. A., Knust, E. and Campos-Ortega, J. A. (1987). The neurogenic gene Delta of *Drosophila melanogaster* is expressed in neurogenic territories ans encodes a putative transmembrane protein with EGF-like repeats. *EMBO J.* **6**, 3431-3440.